Hydraulic Analysis of a Reversible Fluid Coupling

Charles N. McKinnon[1]
Boeing North American,
Downey, CA

Danamichele Brennen[1]
McGettigan Partners,
Philadelphia, PA

Christopher E. Brennen
California Institute of Technology,
Pasadena, CA

ABSTRACT

This paper presents a hydraulic analysis of a fluid coupling which is designed to operate either in a forward or reverse mode when a set of turning vanes are respectively withdrawn or inserted into the flow between the driving and driven rotors. The flow path is subdivided into a set of streamtubes and an iterative method is used to adjust the cross-sectional areas of these streamtubes in order to satisfy radial equilibrium. Though the analyis requires the estimation of a number of loss coefficients, it predicts coupling performance data which are in good agreement with that measured in NAVSSES tests of a large reversible coupling intended for use in a ship drive train.

NOMENCLATURE

A_i	Cross-sectional area of flow at $i = 1, 2, 3$
C_p	Pump torque coefficient, $C_p = T_p/\rho R^5 N_p^2$
C_t	Turbine torque coefficient, $C_t = T_t/\rho R^5 N_p^2$
C_{pw}, C_{tw}	Pump and turbine windage loss coefficients
C_{sw}	Seal windage torque coefficient
C_{pa}, C_{pb}	Pump hydraulic loss coefficients
C_{ta}, C_{tb}	Turbine hydraulic loss coefficients
C_v	Loss coefficient for the turning vanes
H_p, H_{pi}	Actual, ideal total pressure rise across pump
H_t, H_{ti}	Actual, ideal total pressure drop across turbine
H_{pl}, H_{tl}, H_v	Total pressure losses in pump, turbine, turning vanes (non-dimensionalized by $\rho R^2 N_p^2$)
k	Turning vane discharge blockage ratio
N_p, N_t	Angular velocities of the pump, turbine (rad/s)
P_i	Fluid pressure at locations $i = 1, 2, 3$
Q	Volume flow rate of fluid
R	Outer shell radius ($0.5m$)
r_i	Radial position in the flow (m)
r_b	Outer core radius/R
r_c	Inner core radius/R
r_d	Inner shell radius/R
$\bar{r}_{j,i}$	Mean radius of jth streamtube/R
S	Slip $= 1 - N_t/N_p$
T_p, T_t	Shaft torques for the pump, turbine
T_s	Torque in seal between pump + turbine rotors
T_{pw}, T_{tw}	Windage torques for the pump, turbine
u_i	Meridional component of fluid velocity at stations $i = 1, 2, 3$ ($= Q/A_i$)
v_i	Tangential fluid velocity at $i = 1, 2, 3$
$\alpha_p, \alpha_t, \alpha_v$	Angles of attack of flow on pump, turbine, turning vanes (relative to axial plane)
$\beta_p, \beta_t, \beta_v$	Discharge vane angles for pump, turbine, turning vanes (relative to axial plane)
β_v^*	Effective discharge angle for turning vanes
$\delta_p, \delta_t, \delta_v$	Inlet vane angles at pump, turbine, turning vanes (relative to axial plane)
η	Overall coupling efficiency, $\eta = N_t T_t / N_p T_p$
ρ	Fluid density

[1]Formerly with WesTech Gear Corporation, now part of Philadelphia Gear.

1. INTRODUCTION

Fluid couplings and torque converters are now commonly used in a wide variety of applications requiring smooth torque transmission, most notably in automobiles. They usually consist of an input shaft that drives a pump impeller which is closely coupled to a turbine impeller that transmits the torque of an output shaft coaxial with the input shaft. The fluid is usually hydraulic oil and the device is normally equipped with a cooling system to dissipate the heat generated. In a typical fluid coupling used, for example, in a ship propulsion system, the pump and turbine are mounted back to back with little separation between the leading and trailing egdes of the two impellers. It is common to use simple radial blades and a higher solidity (the present pump rotor has 30 vanes) than would be utilized in most conventional pumps or turbines (Stepanoff [1], Brennen [2]). A torque converter as used in automotive transmission systems has an added set of stator vanes mounted between the turbine discharge and the pump inlet.

In the present paper we present a hydraulic analysis of another variant in this class of fluid transmission devices, namely a reversible fluid coupling. This device was developed and built by Franco Tosi in Italy in conjunction with

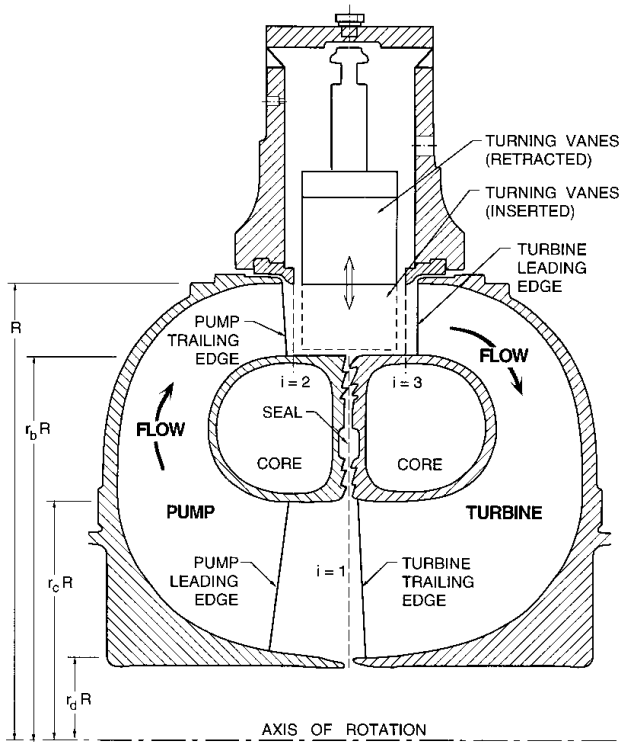

Figure 1: Cross-section of reversible fluid coupling showing key locations in the fluid cavity.

SSS Gears Ltd. in the U.K. and in described in detail in Fortunato and Clements [3], Clements and Fortunato [4] and Clements [5]. Tests on the device conducted by the US Navy (NSWC Philadelphia) and are documented in Nufrio *et al.* [6] (see also, Zekas and Schultz [7]). This paper presents a method of analysis of the performance of such devices and uses one of the Franco Tosi designs tested by NSWC as an example. As shown diagrammatically in figure 1, the reversible fluid coupling has an added feature, namely a set of guide vanes. With the vanes retracted the device operates as a conventional fluid coupling and the direction of rotation of the output shaft is the same as the input shaft. When the vanes are inserted, the direction of rotation of the output shaft is reversed. In traditional terms, the reversible fluid coupling can, in theory, operate over a range of slip values from $S = 0$ to $S = 2$. In the present paper, we utilize overall coupling performance data obtained by NSWC and several investigations of flow details carried out by WesTech Gear Corporation.

A number of recent papers have demonstrated how complex and unsteady the flow is in torque converters (see, for example, By and Lakshminarayana [8], Brun *et al.* [9], Gruver *et al.* [10]. Due, in part, to the need to operate the machines over a wide ranges of slip values, the incidence angles on the impeller blades tend to be very large thus generating substantial flow separation at the leading edges as well as much unsteadiness and high turbulence levels. To accomodate these violent flows and to force the flow to follow the vanes at impeller discharge, the solidity of the impellers is usually much larger than would be optimal in other turbomachines.

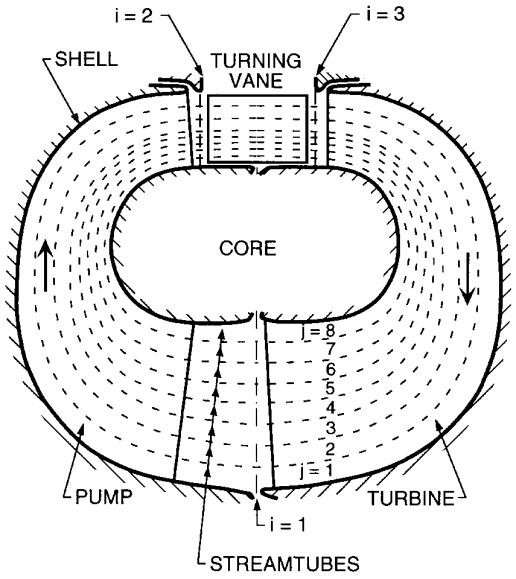

Figure 2: Sketch showing the subdivision of the flow into streamtubes.

Though several efforts have been made to compute these flows from first principles (By *et al.* [11], Schulz *et al.* [12]), such complex, unsteady and turbulent flows with intense secondary flows are very difficult to calculate because of the lack of understanding of unsteady turbulent flows. In the present paper we begin with a simple one-dimensional analysis of the flow in a reversible fluid coupling. This one-dimensional analysis may be used as a first order estimate of the coupling performance. Alternatively it can be applied to a series of streamtubes into which the coupling flow is divided. Such a multiple streamtube (or two-dimensional flow) analysis allows accommodation of the large variations in flow velocity and inclination which occur between the core and the shell of the machine.

In the multiple streamtube analysis the flow is subdivided into streamtubes as shown in figure 2; all the data presented here used ten streamtubes of roughly similar cross-sectional area. The flow in each streamtube is characterized by meridional and tangential components of fluid velocity, u_i and v_i, at each of the transition stations, $i = 1, 2, 3$, between the turbine and the pump ($i = 1$), between the pump and the turning vanes ($i = 2$) and between the turning vanes and the turbine ($i = 3$). A typi-

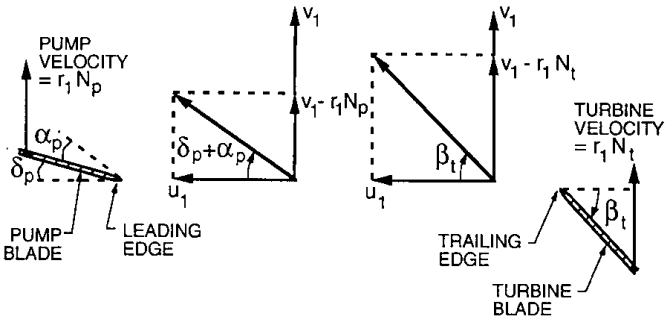

Figure 3: Velocity triangle at the turbine/pump transition station, $i = 1$. Flow is from the right to left, the direction of rotation is upward and the angles are shown as they are when they are positive.

Table 1: Basic geometric data for the reversible coupling.

Pump discharge vane angle, β_p, at shell	$0°$
Pump discharge vane angle, β_p, at core	$0°$
Turbine discharge vane angle, β_t, at shell	$31.5°$
Turbine discharge vane angle, β_t, at core	$44°$
Turning vane discharge angle, β_v	$-55°$
Pump inlet vane angle, δ_p, at shell	$-17°$
Pump inlet vane angle, δ_p, at core	$-10°$
Turbine inlet vane angle, δ_t, at shell	$0°$
Turbine inlet vane angle, δ_t, at core	$0°$
Turning vane inlet angle, δ_v	$55°$
Outer core radius/Outer shell radius, r_b	0.861
Inner core radius/Outer shell radius, r_c	0.592
Inner shell radius/Outer shell radius, r_d	0.29

cal velocity triangle, in this case for the transition station $i = 1$, is included in figure 3; the velocity triangles for the other transition stations are similar.

Later we will present measured performance data for the reversible coupling whose basic geometry is listed in Table 1.

In the multiple streamtube analysis, the mean radius of the jth streamtube (the numbering of the streamtubes is shown in figure 2) at each of the locations $i = 1, 2, 3$ is defined by $\bar{r}_{j,i}$. Since the distribution of velocity will change from one station to the other, only one of these three sets of streamtube radii can be selected *a priori*. We chose to select the series $\bar{r}_{j,1}$ at the turbine/pump transition. It follows that $\bar{r}_{j,2}$ and $\bar{r}_{j,3}$, the streamtube radii at the pump discharge and at the turning vane discharge must then be calculated as a part of the solution. Discussion of how this is accomplished is postponed until the solution methodology is described in section .

2. BASIC EQUATIONS

The process of power transmission through the coupling (operating under steady state conditions) will now be delineated. In the process, several loss mechanisms will be identified and quantified so that a realistic model for the actual interactions between the mechanical and fluid-mechanical aspects of coupling results.

2.1 Pump

The power input to the pump shaft is clearly N_pT_p. Some of this is consumed by windage losses in the fluid annulus between the pump shell and the stationery housing. This is denoted by a pump windage torque, T_{pw}, which will be proportional to N_p^2. Included in this loss will be the shaft seal loss as it has the same functional dependence on pump speed. It is convenient to denote this combined windage and seal torque, T_{pw}, by a dimensionless coefficient, C_{pw}, where $T_{pw} = C_{pw}\rho R^5 N_p^2$. Appropriate vales of C_{pw} can be obtained, for example, from Balje [13] who indicates values of the order of 0.005.

Furthermore the labyrinth seal in the core between the pump and turbine rotors causes direct transmission of torque from the pump shaft to the turbine shaft. This torque which is proportional to $(N_p - N_t)^2$ will be denoted by T_s and is represented by a seal windage torque coefficient, C_{sw}, defined as

$$T_s = C_{sw}\rho R^3(r_b^2 - r_c^2)(N_p - N_t)^2 \qquad (1)$$

A comparison with the experimental data (section 4) suggests a value of C_{sw} of about 0.014. In referring, to this labyrinth seal, we should also observe that the leakage through this seal has been neglected in the present analysis.

It follows that the power available for transmission to the main flow through the pump is $N_p(T_p - T_{pw} - T_s)$ and this manifests itself as an increase in the total pressure of the flow as it passes through the pump. For simplicity, the present discussion will employ a two-dimensional representation of the fluid flow in which the flow is characterized at any point in the circuit by a single meridional velocity, u_i, and a single tangential velocity, v_i, at the appropriate rms radius. In practice, these quantities will vary over the cross section of the flow and this variation is considered later. At this stage it is not necessary to introduce this complexity. The power balance between the mechanical input, the losses and the ideal fluid power applied to the pump, then yields

$$N_p(T_p - T_w - T_s) = QH_{pi} \qquad (2)$$

where, from the application of angular momentum considerations in the steady flow between pump inlet ($i = 1$)

and pump outlet ($i = 2$), the pump head rise, H_{pi}, is given by

$$H_{pi} = \rho N_p (r_2 v_2 - r_1 v_1) \tag{3}$$

More specifically, H_{pi} will be referred to as the ideal pump total pressure rise in the absence of fluid viscosity when the pump would be 100% efficient. However, in a real, viscous flow, the actual total pressure rise produced, H_p, is less than H_{pi}; the deficit is denoted by H_{pl} where

$$H_p = H_{pi} - H_{pl} \tag{4}$$

This total pressure loss, H_{pl}, is difficult to evaluate accurately and is a function, among other things, of the angle of attack on the leading edges of the vanes. Note that the angle of attack, α_p, on the pump blades is given by

$$\alpha_p = tan^{-1} \left\{ \frac{v_1 - r_1 N_p}{u_1} \right\} - \delta_p \tag{5}$$

In the present context the total pressure loss, H_{pl}, is ascribed to two coefficients, C_{pa}, and C_{pb}. The first coefficient, C_{pa}, describes a loss which is a fraction of the dynamic pressure based on the component of relative velocity parallel to the blades at the pump inlet. The second coefficient, C_{pb}, describes a loss which is a fraction of the dynamic pressure based on the component of the pump inlet relative velocity perpendicular to the blades. Thus

$$H_{pl} = \frac{\rho}{2} \left[u_1^2 + (v_1 - r_1 N_p)^2 \right] \left[C_{pa} + (C_{pb} - C_{pa}) sin^2 \alpha_p \right] \tag{6}$$

The coefficients C_{pa} and C_{pb} can be estimated using previous experience in pumps. Though there are many possible representations of the pump total pressure loss, the above form has several advantages. First, at a given flow rate, the loss is appropriately a minimum when α_p is zero, a condition which would correspond to the design point in a conventional pump. And this minimum loss is a function only of C_{pa}. On the other hand at shut-off (zero flow rate) the loss is a function only of C_{pb}. These relations permit fairly ready evaluation of C_{pa} and C_{pb} in conventional pumps given the head rise and efficiency as a function of flow rate. Typical values of C_{pa} and C_{pb} are of the order of unity; but the value of C_{pa} must be less than the value of C_{pb}, the difference representing the effect of the inlet vane angle on the losses in the pump.

The hydraulic efficiency of the pump, η_p, is $1 - H_{pl}/H_{pi}$. In a conventional centrifugal pump for which $v_1 = 0$, the maximum design point efficiency, η_p, is expected to be about 0.85. With the kind of uneven inlet flow to be expected in the present flow a lower value of the order of 0.80 is more realistic. This value provides one relation for C_{pa} and C_{pb}.

2.2 Turbine

We now jump to the turbine output shaft and work back from there. The power delivered to the turbine shaft is $N_t T_t$. As in the pump there are windage losses, $N_t T_{tw}$, where the windage torque, T_{tw}, is described by a dimensionless coefficient, $C_{tw} = T_{tw}/\rho N_t^2$. Then the power delivered to the turbine rotor, $N_t(T_t + T_{tw} - T_s)$, by the main flow through the turbine is related to the ideal total pressure drop through the turbine, H_{ti}, by

$$N_t(T_t + T_{tw} - T_s) = Q H_{ti} \tag{7}$$

where, again, from angular momentum considerations

$$H_{ti} = N_t (r_2 v_3 - r_1 v_1) \tag{8}$$

With an inviscid fluid, H_{ti} would be the actual total pressure drop across the turbine. But in a real turbine the actual total pressure drop is greater by an amount, H_{tl}, which represents the total pressure loss in the turbine, and hence

$$H_t = H_{ti} + H_{tl} \tag{9}$$

In a manner analogous to that in the pump, the total pressure loss in the turbine, H_{tl}, is ascribed to two coefficients C_{ta} and C_{tb}. The first coefficient, C_{ta}, describes a loss which is a fraction of the dynamic pressure based on the component of relative velocity parallel to the blades at the turbine inlet. This coefficient essentially determines the minimum loss at the design point where the angle of attack, α_t, is zero. The second coefficient, C_{tb}, describes a loss which is a fraction of the dynamic pressure based on the component of the turbine inlet velocity perpendicular to the blades. Thus

$$H_{tl} = \frac{\rho}{2} \left[u_3^2 + (v_3 - r_3 N_t)^2 \right] \left[C_{ta} + (C_{tb} - C_{ta}) sin^2 \alpha_t \right] \tag{10}$$

where the the angle of attack, α_t, on the turbine blades is given by

$$\alpha_t = tan^{-1} \left\{ \frac{v_3 - r_2 N_t}{u_3} \right\} - \delta_t \tag{11}$$

As in the case of the pump, appropriate values of C_{ta} and C_{tb} are of the order of unity and should be such as to yield a stand-alone turbine efficiency, H_{ti}/H_t of the order of 0.85. However, C_{tb} must be greater than C_{ta} to reflect the appropriate effect of the inlet vane angles on the hydraulic losses.

2.3 Turning Vanes

The geometry of a turning vane used in the coupling discussed here is shown in figure 4.

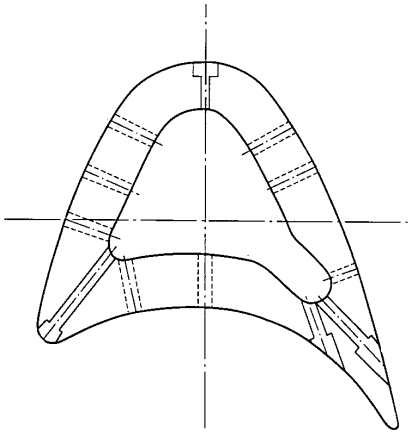

Figure 4: Cross-section of a turning vane.

The total pressure rise produced by the pump, H_p, is equal to the total pressure drop across the turbine, H_t, plus the total pressure drop across the turning vanes, H_v, so that

$$H_p = H_t + H_v \quad \text{with the turning vanes inserted} \tag{12}$$

$$H_v = 0 \quad \text{with the turning vanes retracted} \tag{13}$$

It is this balance which essentially determines the flow rate, Q, and the meridional velocities, u_i. The total pressure drop across the vanes, H_v, is described a loss coefficient defined by

$$C_v = 2H_v/\rho(v_3^2 + u_3^2) \tag{14}$$

Though both H_v and C_v will vary with the angle of attack of the flow on the turning vanes, α_v, we have not exercised that option here since there is no independent information on the turning vane performance. Estimates from experience suggest that C_v should lie somewhere between about 0.3 and 1.0.

2.4 Turbine Partial Admission Effect

Due to the large blockage effects of the turning vanes, the flow discharging from the vanes consists of an array of jets interspersed with relatively stagnant vane wakes. This means that during reverse operation the turbine experiences inlet conditions similar to those in a partial admission turbine. In the hydraulic analysis we can approximately account for these partial admission effects by taking note of the following property of partial admission. Consider and compare the flux of angular momentum in the flow into the turbine, first, for full admission and, second, for partial admission. Under uniform, full admission conditions, u_3 and v_3 are independent of circumferential position and the flux of angular momentum entering the turbine is proportional to $u_3 v_3$. If the swirl angle were defined by the turning vane discharge angle then this reduces to $u_3^2 \tan\beta_v$. On the other hand a partial admission flow consisting of jets with velocity components u_3^*, v_3^* alternating with stagnant wakes of zero velocity would have a flux of angular momentum equal to $k u_3^* v_3^*$ where k is the fraction of the cross-sectional area occupied by the jets ($0 < k < 1$). But if the total flow rate is the same in both cases then $u_3^* = u_3/k$ and if the jets are parallel with the turning vane discharge angle then $v_3^* = u_3^* \tan\beta_v$. Hence the flux of angular momentum becomes $u_3^2 \tan\beta_v/k$. In other words the blockage which creates the jets and wakes also leads to an *increase* in the flux of angular momentum by the factor, $1/k$.

To account for this in the flow analysis, the appropriate angular momentum flux (which is essential to the basic principles of the pump or turbine) can be maintained by inputting an *effective* turning vane discharge angle denoted by β_v^*. Comparing the above expressions the effective turning vane discharge angle is given by

$$\tan\beta_v^* = \tan\beta_v/k \tag{15}$$

Hence by inputting a somewhat larger than actual turning vane discharge angle we can account for these partial admission effects.

The problem therefore reduces to estimating an appropriate value for k from the experimental measurements. For this purpose, we develop the relation between k and the loss coefficient for the turning vanes, C_v. If the total head of the jets is assumed to be equal to the upstream total head (at location $i = 2$), then it is readily shown that the *mean* total head of the discharge (including the wakes) implies the following relation between k and C_v:

$$k = \left\{ \frac{1 - C_v tan^2\beta_v}{1 + C_v} \right\}^{\frac{1}{2}} \tag{16}$$

The value of $C_v = 0.36$ which is deployed later along with the appropriate $\beta_v = -55°$ yield $\beta_v^* = -72.8°$ and a blockage ratio (or partial emission factor) of $k = 0.44$ which seems reasonable given the geometry of the turning vane cascade.

3. SOLUTION OF THE FLOW

3.1 Solution for an individual streamtube

Consider first the solution of the flow in an individual streamtube where it is assumed that the velocity at any location in the circular path (figure 2) can be characterized by a single meridional and a single tangential velocity.

Assume for the moment that the radial positions of the streamtube are known; then the inlet and discharge angles encountered by that particular streamtube at those radial positions at each of the transition stations can be determined. Then for a given slip, $S = 1 - N_t/N_p$, the first step is to solve the flow equation (12) or more specifically:

$$H_{pi} - H_{pl} = H_{ti} + H_{tl} + H_v \tag{17}$$

to obtain the flow rate and velocities. The procedure used starts with a trial value of u_1. Values of u_2, u_3 follow from continuity knowing the areas A_i:

$$u_i = u_1 A_1/A_i \quad , \quad i = 2, 3 \tag{18}$$

Furthermore, it is assumed that the relative velocity of the flow discharging from the pump, the turning vanes or the turbine is parallel with the blades of the respective device (or the effective angle in the case of the turning vanes). Given the high solidity of the pump and turbine, this is an accurate assumption. This allows evaluation of the tangential velocities:

$$v_1 = r_1 N_t + u_1 \tan\beta_t \tag{19}$$

$$v_2 = r_2 N_p + u_2 \tan\beta_p \tag{20}$$

where r_1 and r_2 are rms channel radii at each location and $v_3 = v_2$ for the turning vanes retracted and $v_3 = u_3 \tan\beta_v$ for the turning vanes inserted. These relations can then be substituted into the definitions (3), (8), (6), (10) and (14) to allow evaluation of all the terms in equation (17). That equation is not necessarily satisfied by the initial trial value for u_1. Hence an iteration loop is executed to find that value of u_1 which does satisfy equation (17). The velocities and flow rate are thus determined for a given value of the slip.

3.2 Multiple Streamtube Solution

As described in the last section, the multiple streamtube analysis begins with a set of guessed values for the streamtube locations at the transition stations, $i = 2$ and $i = 3$. It also begins with an assumed value for the flowrate in each streamtube (more specifically an assumed value of $u_1 = 1$.) Then the method of the last section is used to solve for the flow and allows evaluation of the total pressure changes and losses in each streamtube. Then, the degree to which equation (17) is satisfied is assessed. This leads to an improved value of u_1 and the process is repeated to convergence (only three or four cycles are necessary). By doing this for each streamtube we obtain the total pressure and the static pressure differences between all three locations for each streamtube.

Table 2: Power transmission and losses.

Pump shaft power	$= N_p T_p$
Power lost in pump windage	$= N_p T_{pw}$
Power to turbine through seal	$= N_p T_s$
Power to main pump flow	$= Q H_{pi}$
	$= N_p(T_p - T_{pw} - T_s)$
Power in main flow out of pump	$= Q(H_{pi} - H_{pl})$
Power lost in turning vanes	$= Q H_v$
Power in flow entering turbine	$= Q(H_{pi} - H_{pl} - H_v)$
	$= Q(H_{ti} + H_{tl})$
Power to turbine rotor by flow	$= Q H_{ti}$
	$= N_t(T_t + T_{tw} - T_s)$
Power to turbine through seal	$= N_t T_s$
Power lost in turbine windage	$= N_t T_{tw}$
Turbine shaft power	$= N_t T_t$

The principle by which the streamtube geometry is adjusted is that the flows in each of the three locations should be in radial equilibrium. This implies that, at each of the locations $i = 1, 2, 3$, the flow must satisfy

$$\left(\frac{\partial P}{\partial r}\right)_i = \frac{\rho v_i^2}{r_i} \tag{21}$$

where P is the static pressure. Application of this condition at the turbine/pump transition station ($i = 1$) establishes the static pressure difference between each streamtube. Then using the information from the flow solution on the static pressure differences between transition stations we can establish the pressure distribution between the streamtubes at transition stations $i = 2$ and $i = 3$. Then using equation (21) we examine whether the flows in these locations are in radial equilibrium. Given the initial trial values of $\bar{r}_{j,2}$ and $\bar{r}_{j,3}$, this will not, in general, be true. The method adjusts the values of $\bar{r}_{j,2}$ and $\bar{r}_{j,3}$ and then repeats the entire process until radial equilibrium is indeed achieved at transition stations $i = 2$ and $i = 3$. This requires as many as 30 iterations.

3.3 Power Transmission Summary

This completes the description of the power transmission through the coupling which is summarized in Table 2. The overall efficiency of the coupling, η, is given by

$$\eta = \frac{N_t T_t}{N_p T_p} = \frac{Q H_{ti} - N_t T_{tw} + N_p T_s}{Q H_{pi} + N_p T_{pw} + N_p T_s} \tag{22}$$

or substituting from equations (4) and (9):

$$\eta = \frac{N_t(r_2 v_3 - r_1 v_1) - (N_t T_{tw} + N_t T_s)/Q}{N_p(r_2 v_2 - r_1 v_1) + (N_p T_{pw} + N_p T_s)/Q} \tag{23}$$

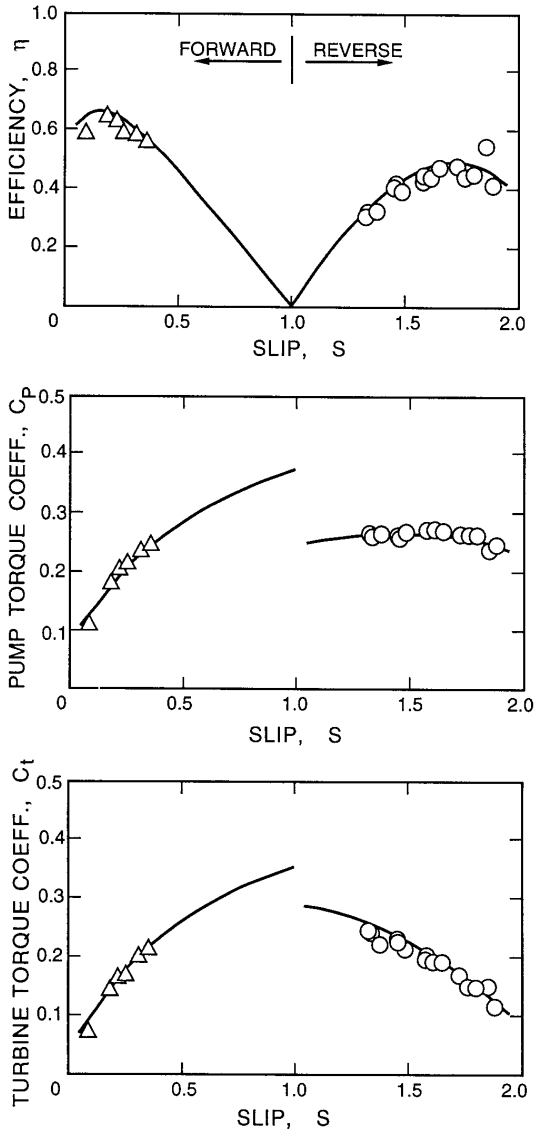

Figure 5: Efficiency and torque coefficients for the reversible coupling using $C_{pa} = C_{ta} = 0.7$, $C_{pb} = C_{tb} = 1.0$, $C_v = 0.36$, $C_{sw} = 0.02$, $C_w = 0.005$ and an effective turning vane discharge angle of $-72.8°$.

This expression demonstrates an important feature of the reversible coupling. In the forward mode with the vanes removed, $v_2 = v_3$, and the quantities in parentheses in the numerator and denominator are identical. Therefore, if the windage torques, T_{tw} and T_{pw}, are small as is normally the case and if Q is not close to zero (as can only happen close to $S = 0$) then the coupling efficiency is close to $N_t/N_p = 1 - S$. Thus, in the forward mode, only the windage losses cause the efficiency to deviate from $1 - S$. On the other hand no such simple relation exists in the reverse mode.

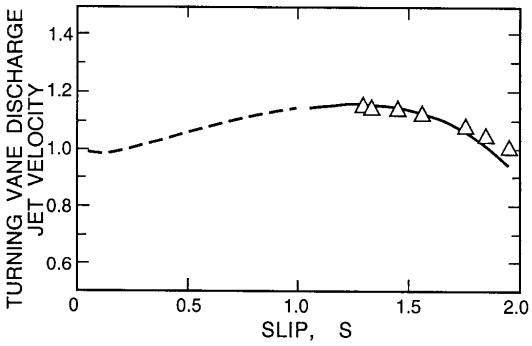

Figure 6: Velocity of turning vane discharge jets for the same conditions as listed in figure 5.

Apart from the overall efficiency, η, two other coupling characteristics will be presented, namely the pump torque coefficient, C_p, and the turbine torque coefficient, C_t. Note the choice of N_p in the denominator for C_t.

4. COMPARISON WITH EXPERIMENTS

4.1 Experimental Data

The efficiency, torque coefficients and fluid velocities measured during tests of the coupling conducted by NAVSSES (using an oil of density 849 kg/m^3) at a input (or pump) speed of $1000rpm$ will be compared to the results of the present analytical model. Note that although three graphs for η, C_p and C_t are presented, these only represent two independent sets of data since $\eta = C_t(1 - S)/C_p$.

4.2 Performance

A typical set of results for the performance of the coupling are presented in figures 5 and 6. The coefficients C_{pa}, C_{pb}, C_{ta}, C_{tb}, and C_{va} (and, to a lesser extent, C_w and C_{sw}) were chosen to match the experimental data by proceeding as follows. First note that C_w and C_{sw} have little effect *except* close to $S = 0$. In fact, the peak in η near $S = 0$ is almost entirely determined by C_w and values of $C_w = 0.02$ were found to fit the data near $S = 0$ quite well. This value is also consistent with previous experience on windage coefficients (Balje [13]). Similarly past experience would suggest a value of 0.005 for the seal windage coefficient, C_{sw}.

Turning to the pump, turbine and turning vane loss coefficients, it is clear that the turning vanes have no effect on forward performance ($S < 1$). Hence the pump and turbine loss coefficients were chosen to match this data. In

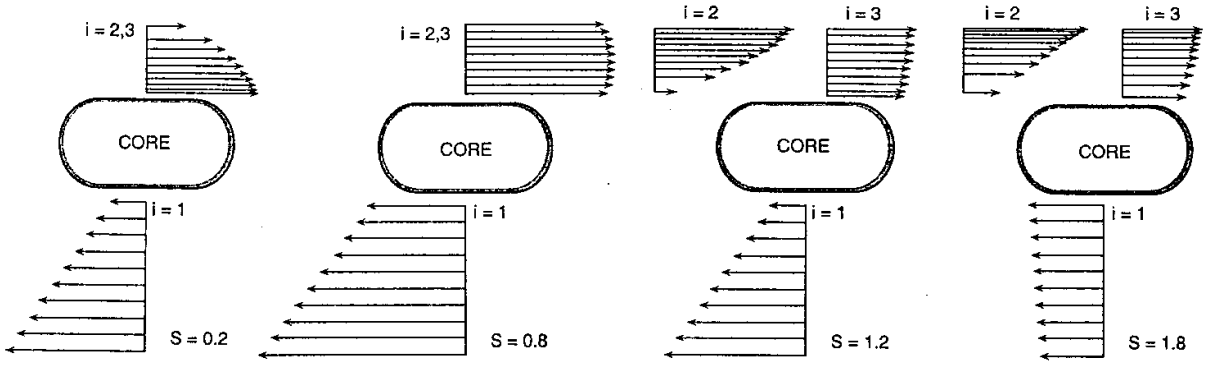

Figure 7: Meridional velocity distributions at the transition stations for four different slip values.

this regard the efficiency is of little value since the forward efficiency is always close to $(1-S)$. Values of $C_{pa} = C_{ta} = 0.7$ and $C_{pb} = C_{tb} = 1.0$ seemed to match the forward torque coefficients well. These could be supported by the argument that all the dynamic head normal to the vanes at inlet will likely be lost (thus $C_{pb} = C_{tb} = 1.0$) and a high fraction of that parallel with the vanes is also likely to be lost (thus $C_{pa} = C_{ta} = 0.7$). Note that the results presented are not very sensitive to the precise values used for these loss coefficients. It should also be noted that these loss coefficients yield sensible peak efficiencies for the pump or turbine when these are evaluated for stand-alone performance (respectively 79% and 86%).

Finally, then, we turn to the reverse performance ($S > 1$) with only one loss coefficient left to determine, namely the loss due to the turning vanes, C_{va}. In the example shown a value of C_{va} of 0.36 yields values of the efficiency which are consistent with the experimental results.

Note that if the coefficients described above were used with the actual turning vane discharge angle, there would be substantial discrepancies between the observed and calculated results; this helps to confirm the analysis of section and the use of the effective turning vane discharge angle, $\beta_v^* = -72.8°$.

4.3 Velocity Distributions

The multiple streamtube approach also provides information on the distributions of flow, angles of attack, etc. within the coupling and demonstrates how these change with slip. Examination of the results revealed several ubiqitous non-uniformities and one example, presented in figure 7, will suffice to illustrate these. At low slip values in forward operation the meridional velocity profiles are very non-uniform. This non-uniformity consists of much higher meridional velocities near the axis in the turbine-to-pump transition and at the outer radius in all the transitions. As the slip increases in forward operation this non-uniformity decreases; near $S = 1$ it has disappeared at the pump-to-turbine transition but remains at the turbine-to-pump transition. When the turning vanes are inserted, the velocity profiles show a highly non-uniform character in the pump-to-turning-vane transition but this is almost completely evened out by the turning vanes. The turbine-to-pump non-uniformity near $S = 1$ is not too dissimilar to that in forward operation near $S = 1$. However, it is interesting to note that this non-uniformity is reversed as $S = 2$ is approached. These changing non-uniformities are important becaause they imply corresponding changes in the distribution of the angles of attack on the pump, turning vanes, and turbine. Consequently, the optimal vane inclination distributions (which would have as their objective uniform angles of attack) are different for forward and reverse operation.

5. CONCLUSIONS

This paper presents a hydraulic analysis of a reversible fluid coupling operating over a range of slip values in both forward ($0 < S < 1$) and reverse ($1 < S < 2$) operation. The analysis employs estimates loss coefficients for the pump, turbine, turning vanes, windage and core seal. It splits the flow into an array of streamtubes with pressure balancing adjustment across those streamtubes and solves to find the fluid velocities, flow rate and static pressures at each of the transition stations for each streamtube. This information then allows evaluation of the overall performance characteristics including the efficiency and the pump and turbine torque coefficients. Comparison with data from the full scale testing (conducted by the US Navy) of a reversible fluid coupling made by Franco-Tosi demonstrates good agreement between the analysis and the experiments. While the analysis involves the selection and identification of a number of hydraulic loss

coefficients, the values of the coefficients do appear to be valid over a wide range of operating points, slip values and speeds. Moreover, though these coefficients are necessarily specific to the particular coupling studied, they nevertheless provide benchmark guidance for this general class of machine.

When the coupling is operated in the forward mode, the flow rates are small and hence the hydraulic losses are quite minor. Thus the efficiency is close to the ideal. However, as the slip increases, the flow rates become larger and the hydraulic losses (which increase like the square of the flowrate) become substantial. Under these conditions the device behaves much more like an interconnected pump and turbine than a conventional fluid coupling and the overall efficiency is similar to that one would expect from a device which links drive trains through a combination of a pump and a turbine. Even under the best of circumstances the analysis suggests that the efficiency of this generic type of coupling could not be expected to exceed 60% in the reverse mode.

The analysis presented here also demonstrates that, since it is used over a wide range of slip values, a reversible fluid coupling must operate over a wide range of angles of attack of the flows entering the pump and turbine rotors. With fixed geometry rotors, this inevitably results in substantial hydraulic losses, particularly in the reverse mode. Choosing the inlet blade angles in order to minimize those losses is not simple and it is not clear how the fixed geometry should be chosen in order to achieve that end.

ACKNOWLEDGEMENTS

The analyses described were performed for WesTech Gear Corporation, now part of Philadelphia Gear, and the authors are very grateful to both organizations for their concurrence in the publication of this paper. We are also very appreciative of the help and advice of Tom Gugliuzza of WesTech Gear.

REFERENCES

[1] Stepanoff, A.J., 1957, "*Centrifugal and axial flow pumps*," John Wiley and Sons, Inc.

[2] Brennen, C.E., 1994, "*Hydrodynamics of Pumps*," Oxford University Press and Concepts ETI, Inc.

[3] Fortunato, E. and Clements, H.A., 1979, "Marine reversing gear incorporating single reversing hydraulic coupling and direct-drive clutch for each turbine," *ASME Paper No. 79-GT-61.*

[4] Clements, H.A. and Fortunato, E., 1982, "An advance in reversing transmissions for ship propulsion," *ASME Paper No. 82-GT-313.*

[5] Clements, H.A., 1989, "Stopping and reversing high power ships," *ASME Paper No. 89-GT-231.*

[6] Nufrio, R., Schultz, A.N. and McKinnon, C.N., 1987, "Final report - reverse reduction gear/reversible converter coupling test and evaluation," PM-1500B.

[7] Zekas, B.M. and Schultz, A.N., 1997, "Unique reverse and maneuvering features of the AOE-6 reverse reduction gear," *ASME Paper No. 97-GT-515.*

[8] By, R.R. and Lakshminarayana, B., 1995, "Measurement and analysis of static pressure field in a torque converter pump," *ASME J. Fluids Eng.*, **117**, pp. 109–115.

[9] Brun, K., Flack, R.D. and Gruver, J.K., 1996, "Laser velocimeter measurements in the pump of an automotive torque converter. Part II - Unsteady measurements," *ASME J. Fluids Eng.*, **118**, pp. 570–577.

[10] Gruver, J.K., Flack, R.D. and Brun, K., 1996, "Laser velocimeter measurements in the pump of an automotive torque converter. Part I - Average measurements," *ASME J. Fluids Eng.*, **118**, pp. 562–569.

[11] By, R.R., Kunz, R. and Lakshminarayana, B., 1995, "Navier-Stokes analysis of the pump flow field of an automotive torque converter," *ASME J. Fluids Eng.*, **117**, pp. 116–122.

[12] Schulz, H., Greim, R. and Volgmann, W., 1996, "Calculation of three-dimensional viscous flow in hydrodynamic torque converters," *ASME J. Fluids Eng.*, **118**, pp. 578–589.

[13] Balje, O.E., 1981, "*Turbomachines. A guide to design, selection and theory*," John Wiley and Sons, New York.